*Journal of the European Ceramic Society* **18** (1998) 1493–1502
© 1998 Elsevier Science Limited
Printed in Great Britain. All rights reserved
PII: S0955-2219(98)00082-X
0955-2219/98/$—see front matter

# The Adsorption of Tri Alkoxy Silane on Silicon Nitride for Colloidal Processing

Joseph A. Yanez,[a]* Brigitte Baretzky,[b] Manfred Wagner[c] and Wolfgang M. Sigmund[a]

[a]Max-Planck-Institut für Metallforschung Abteilung Aldinger, Heisenbergstraße 5, 70569 Stuttgart, Germany
[b]Max-Planck-Institut für Metallforschung, Seestraße 92, 70174 Stuttgart, Germany
[c]Max-Planck-Institut für Polymerforschung, D-55021 Mainz Postfach 3148, Germany

(Received 19 August 1997; accepted 25 February 1998)

***Abstract***

*$^{29}Si$ NMR, diffuse reflectance infrared fourier transform (DRIFT) spectroscopy, X-ray photoelectron spectroscopy (XPS), ultraviolet spectroscopy (UV), ellipsometry, and atomic force microscopy (AFM) measurements were used to characterize the interaction of N–(triethoxysilylpropyl)–O–poly–ethylene oxide urethane with a $Si_3N_4$ surface in water. The experimental results show that this tri alkoxy silane molecule covalently bonds to the surface of $Si_3N_4$. Maximum adsorption of this compound was $2{\cdot}13\ \mu mol\ m^{-2}$, but less than $0{\cdot}1\ \mu mol\ m^{-2}$ of this amount is chemically grafted to the surface. However, AFM results show that such a low amount of material is sufficient to increase the repulsive potential between $Si_3N_4$ surfaces. © 1998 Elsevier Science Limited. All rights reserved*

## 1 Introduction

Because of its low coefficient of thermal expansion and high fracture toughness, components manufactured from silicon nitride are of great interest for engine parts, cutting tools,[1] and other applications[2] which require high heat-resistance and wear-resistance. These types of components require high performance and high reliability which are properties not normally attributed to ceramic materials. Colloidal ceramic processing,[3,4] has the potential to remove or minimize the flaw populations responsible for low Weibull moduli and poor fracture toughness. Material properties are improved by the removal of strength limiting heterogeneities by filtration. In this method, the ceramic powder is first dispersed in a medium. For environmental and economic reasons, an aqueous medium is preferred. When the particles are first dispersed in the medium the volume fraction of particles should be low and the interparticle potential highly repulsive, so that the pressure needed to filter the suspension is minimal. After removing the heterogeneities and prior to consolidation to a higher volume fraction, the interparticle potential should be changed to a weakly attractive potential (i.e. short range repulsive potential). The weakly attractive potential is necessary for three reasons. First, it will prevent mass segregation in suspensions of different phases during consolidation.[5] Second, it allows a mechanism to alleviate residual stress introduced during consolidation.[6] Third, particle suspensions with a weakly attractive potential possess a yield stress and thus bodies can be reformed into a desired shape after consolidation.[7]

A short range repulsive potential between ceramic particles can be produced by many different techniques.[8–10] All methods involve some variation of truncating the attractive van der Waals potential.[11] One such method is by adsorbing molecules on the surfaces of the particles.[12] The adsorbed molecules produce a brush-like structure on the surface which limits the closest separation distance of the particles to twice the length of the adsorbed molecule. Varying the length of the adsorbed chain, changes the magnitude of the truncation of the attractive van der Waals potential and thus the strength of interaction between particles.[12] The longer the adsorbed molecule the weaker the attraction between particles. At some characteristic length, the interparticle potential will become purely repulsive. The characteristic length will depend on the Hamaker constant of the material being dispersed. For materials with larger

*To whom correspondence should be addressed.

Hamaker constants, longer chain lengths will be needed to achieve colloidal stability.

One difficulty that often arises during powder consolidation is the desorption of organic aids from the surface.[13] This desorption removes the short range repulsive force and allows particles to come into contact, negating some of the advantages of the colloidal processing method. Therefore, it is necessary to use very strongly physically or chemically adsorbed molecules. Kramer *et al.*[14] have shown that it is possible to chemically graft alcohol chains of varying length onto the surface of silicon nitride. However, the alcohol chains cause the particles to be hydrophobic and thus not soluble in the preferred aqueous medium.

Recently, Buchta *et al.*[15] and Colic *et al.*[16] used silane molecules to disperse silicon nitride in water. These molecules provided the desired short range repulsive force and did not desorb during consolidation. In addition, their results suggested that the silane molecules prevented dissolution of the silica from the surface of the particles.

Tri alkoxy silane molecules have been used for years in the adhesion industry as coupling agents.[17–19] The R group and the X group can be altered depending on the desired application. Upon addition to water the alkoxy groups hydrolyze to form silanols, eqn (1). This hydrolysis reaction is rapid in an acidic environment. The tri alkoxy silane molecule can then polymerize by reacting with other silanol groups, eqn (2).

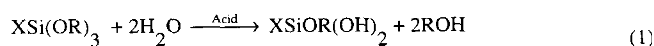

$$XSi(OR)_3 + 2H_2O \xrightarrow{Acid} XSiOR(OH)_2 + 2ROH \quad (1)$$

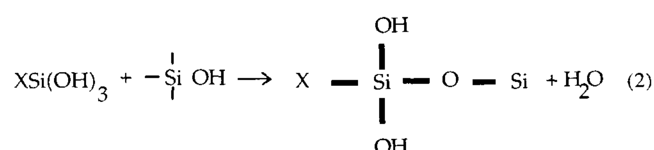

$$XSi(OH)_3 + -Si\,OH \rightarrow X - Si(OH)_2 - O - Si + H_2O \quad (2)$$

It is well documented[20,21] that the amine groups on the surface of $Si_3N_4$ react with water to form silanol groups, eqn (3).

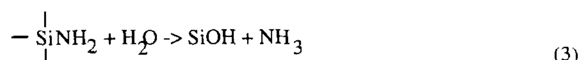

$$-SiNH_2 + H_2O \rightarrow SiOH + NH_3 \quad (3)$$

Buchta *et al.*[14] had the novel idea that the tri alkoxy silane molecule would react with the silanol molecules on the surface of $Si_3N_4$, forming the much desired chemical bond [eqn (2)]. The length of the adsorbed chain can be varied by altering the length of the X-group.

This paper will attempt to characterize the interaction of a tri alkoxy silane molecule with a $Si_3N_4$ surface and determine its effect on the interparticle potential. $^{29}Si$ NMR was used to characterize the starting compound as well as the compounds formed upon hydrolysis and then condensation. Diffuse reflectance infrared fourier transform (DRIFT) spectroscopy and X-ray photoelectron spectroscopy (XPS) were used to characterize how the tri alkoxy molecule bonds to the surface of silicon nitride. Ultraviolet spectroscopy (UV) and ellipsometry measurements were used to determine the amount of adsorbed material. Atomic force microscopy (AFM) measurements of force versus separation distance were used to determine the effect of the tri alkoxy silane molecule on the interparticle potential.

## 2 Materials

The silane molecule used in this study was N–(triethoxysilylpropyl)–O–poly–ethylene oxide urethane (Gelest Inc. (ABCR), Germany), Fig. 1, and will be referred to as PEO silane. This was one of the compounds explored by Colic *et al.*[16] This compound was used as received. In a fully extended all-trans conformation the hydrolyzed molecule has a length of approximately 2·2 nm. The $Si_3N_4$ powder used for the UV adsorption studies and DRIFT measurements was UBE E03 ($d_{50} = 1{\cdot}21\ \mu m$). Polished substrates for AFM and XPS studies were made from gas pressure sintered $Si_3N_4$ bodies with 8 wt% (3 wt% $Al_2O_3$ and 5 wt% $Y_2O_3$) sintering aids. Polished substrates suitable for ellipsometry measurements were prepared from hot isostatic pressed $Si_3N_4$ bodies with 2 wt% ($Al_2O_3$ and $Y_2O_3$) sintering aids.

## 3 Experimental

### 3.1 NMR

Samples were analyzed by $^{29}Si$ NMR spectroscopy using a Bruker spectrometer DRX 500 (Karlsruhe, Germany), operating at a frequency of 90·34 MHz. Spectra were run at 25°C. The field width was 15 kHz, the sequence delay (d1) 30 s, and the pulse sequence was inversed gated decoupling. Two samples were prepared, PEO silane in deuterated tetrahydrofuran (THF) and PEO silane in $D_2O$ with HCl . A 4 to 1 ratio of solvent to PEO silane was used. Samples were prepared 24 h before taking the spectra. The following nomenclature, $T_x^y$,

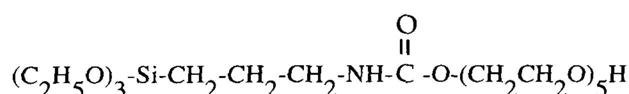

$$(C_2H_5O)_3\text{-}Si\text{-}CH_2\text{-}CH_2\text{-}CH_2\text{-}NH\text{-}C(=O)\text{-}O\text{-}(CH_2CH_2O)_5H$$

**Fig. 1.** Molecular structure of N–(triethoxysilylpropyl)–O–poly–ethylene oxide urethane.

will be used to describe the chemical environment of the silicon atom. The superscript y denotes that a bond has formed by a condensation reaction and the subscript x denotes that a silanol has formed by hydrolysis. x and y must not exceed 3. Figure 2 shows an example of a $T_1^1$ silicon atom.

### 3.2 Drift

Diffuse reflectance infrared fourier transform (DRIFT) spectroscopy measurements were made with a Bruker (Karlsruhe, Germany) Infrared Spectrometer 66 with a diffuse reflectance accessory from Harrick Scientific Instruments (Ossning, NY, USA). Samples were prepared by dispersing the silicon nitride powder in water (pH 2) with (0·25 wt%) and without PEO silane. The suspensions were allowed to equilibrate for 24 h and then centrifuged to remove the solvent. The powder was then rinsed with deionized water and allowed to dry. The rinsing and drying procedure was repeated five times. Measurements were done at room temperature.

### 3.3 XPS

The surface composition and concentration of a PEO-Silane film on a $Si_3N_4$ substrate as well as the substrate itself were analyzed by X-ray photoelectron spectroscopy (XPS).[22–24] In order to prevent a degradation of the organic film, a special handling procedure was followed: The polished substrate was allowed to remain in the PEO silane solution (0·25 wt%) until just before measurement. After only a short drying time the sample was put into a vacuum pre-chamber for an outgassing time of 48 h at a base pressure of approximately $1 \times 10^{-5}$ Pa. The samples were then transferred into the main UHV-chamber with a base pressure of $3 \times 10^{-7}$ Pa. The XPS measurements were performed with a Perkin-Elmer Φ5300 spectrometer, using a Mg-$K_\alpha$ X-ray source with an electron acceleration energy of 12 kV and a power of 300 W.

The photoelectrons, emitted from the Si 2s, the Si 2p, the C 1s, the N 1s and O 1s levels, were measured at a take-off angle of 45°, relative to the surface with a concentric hemispherical analyzer. A pass energy of 89·5 eV was used for the survey spectra and a pass energy of 71·55 eV for the multiplex (narrow scan) spectra. In order to analyze the near-surface concentration, the take off angle

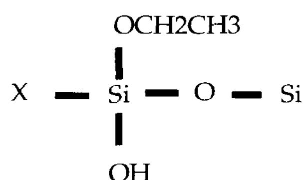


**Fig. 2.** Example of a $T_1^1$ silica atom.

(Ψ) was varied stepwise between 15° and 45° relative to the surface. Decreasing the take-off angle (Ψ) of the emitted photoelectron, results in a decrease of the information depth. Thus, signals from the outer layer (e.g. the polymer film) are more pronounced. Since X-ray bombardment is known to degrade organics, acquisition time was reduced at the expense of the signal-to-noise ratio.

In order to acquire a standard for comparison, an untreated $Si_3N_4$ substrate was analyzed. The sample was found to have a 'natural' surface contamination layer, which was sputtered off by 3 KeV $Ar^+$ bombardment after approximately 24 min.

### 3.4 UV adsorption isotherm

PEO silane was determined to be UV active at a wavelength of 212 nm. A calibration curve was generated by determining the UV adsorption in transmission for known amounts of PEO silane. Samples were prepared by dispersing a fixed volume fraction of silicon nitride powder in water (pH 10) with various concentrations of PEO silane. The samples were vigorously shaken for 24 h and then the powder and solvent were separated by centrifugation. The supernate was analyzed to determine the amount of PEO silane. The difference of the starting concentration and the concentration in the supernate was determined to be the amount adsorbed.

### 3.5 Ellipsometry

The measurements were performed using a null ellipsometer manufactured by Optrel (Berlin, Germany). All measurements shown were taken with a He-Ne laser with a wavelength of 632·8 nm. Adsorption isotherms were determined as follows: The polished sample was placed into a specially designed glass cell. The cell was then filled with deionized water at pH 10. The stability of the system was then checked. A concentrated solution of PEO silanol was then added and the system was allowed to reach equilibrium. The concentrated solution was prepared at pH 10. An isotherm curve was obtained by systematically increasing the PEO silanol concentration while recording the ellipsometric angles Δ and Ψ. It was assumed that the system was comprised of three layers, $Si_3N_4$, $SiO_2$, and PEO silane. For the four different samples explored, the layer of $SiO_2$ between the bulk $Si_3N_4$ sample and the PEO silane film varied between 12 and 25 angstroms. The Fresnel equations were then solved using the software provided by Optrel to determine the index of refraction and the film thickness for each concentration. Equation (4) was then used to determine the amount of adsorbed compound, A (mg $m^{-2}$).

$$A = d_l(n_l - n_0)/(dn/dc) \quad (4)$$

$d_l$ is the calculated layer thickness and $n_l$ is the refractive index of the adsorbed film, $n_0$ is the refractive index of the pure water and $dn/dc$ is the refractive index increment of PEO Silanol in water. It has been determined on an Abbe refractometer that $dn/dc = 1{\cdot}225 \times 10^{-4}$ ml mg$^{-1}$.

### 3.6 Atomic force microscopy

Interparticle forces were measured in a closed liquid cell using a Digital Instruments Multimode Nanoscope III atomic force microscope (Santa Barbara, CA, USA). The standard cantilever for this AFM is made of $Si_3N_4$. Solutions of deionized water and $1 \times 10^{-3}$ g ml$^{-1}$ PEO silane were prepared at pH 10. The substrate was loaded into the liquid cell, filled with deionized water, and then the interparticle forces between the $Si_3N_4$ substrate and the $Si_3N_4$ AFM tip were measured. The interparticle potential with $1 \times 10^{-3}$ g ml PEO silane was measured in the same way. A description of the analysis of the force-distance curves is given elsewhere.[25]

## 4 Report and Discussion of Experimental Results

### 4.1 NMR

Figure 3 shows $^{29}$Si NMR spectra of PEO Silane in THF. Since the THF contains no water, hydrolysis of the compound should not take place and the results should show the starting compound. Figure 3 shows that no polymerization has occurred in the starting compound (i.e. y = 0). Hence, the as received PEO silane from Gelest consists of only $T_0{}^0$ (46 ppm), $T_1{}^0$ (45·78 ppm), $T_2{}^0$ (45·56 ppm) silica molecules, Fig. 3. It is possible that the peak for $T_0{}^0$ is the peak for $T_1{}^0$ and $T_1{}^0$ is $T_2{}^0$ and $T_2{}^0$ is $T_3{}^0$, but three free silanol groups would be extremely reactive and the spectra shows no Si–O–Si bonds. Hence, we conclude that there is no $T_3{}^0$. Integration of the peaks shows that the as received PEO silane is comprised of 41·8% of $T_0{}^0$, 37·2% of $T_1{}^0$, and 21% of $T_2{}^0$, Fig. 4.

Figure 5 shows the spectra for PEO silane dissolved in $D_2O$ with HCl added. Without the addition of HCl, the PEO silane and $D_2O$ initially phase separated. The kinetics of the reaction given by eqn (2) are greater reduced at higher pH. When HCl was added the solution rapidly became fully soluble. Figure 5 shows that PEO silane in $D_2O$ undergoes polycondensation reactions [eqn (2)] to form $T_x{}^1$ (51·09 ppm), $T_x{}^2$ (59·958 ppm), and (67·65 ppm) siloxane molecules. Non-condensated Si molecules, $T_x{}^0$ (41·48 ppm), are also still present in solution. Integration of the peaks shows that the solution is comprised of 9% of $T_x{}^1$, 53% of $T_x{}^2$, 37% of $T^3$, and 1% $T_x{}^0$. The broad peak around 110 ppm is the peak signal for the tube glass.

### 4.2 Drift

Figure 6(a) shows the entire DRIFT spectra for uncoated and PEO coated silicon nitride powder. The peaks at low wave number are attributed to the powder. Figure 6 (insert) shows an enlargement

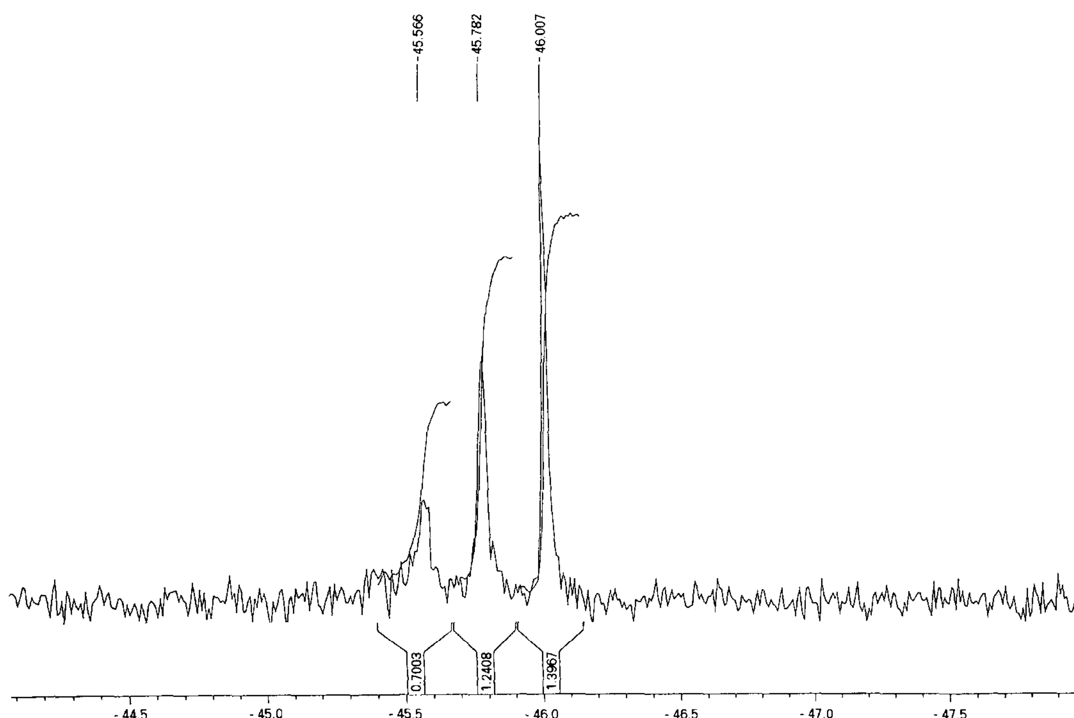


**Fig. 3.** $^{29}$Si NMR spectra of PEO silane in deuterated THF.

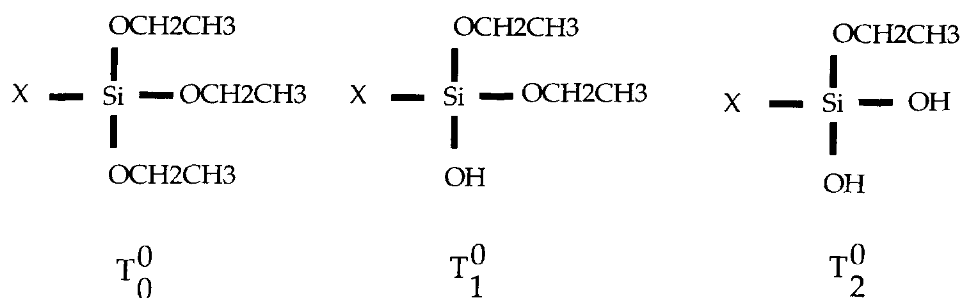


**Fig. 4.** Structures of $T_0{}^0$, $T_1{}^0$, and $T_2{}^0$ silica atoms.

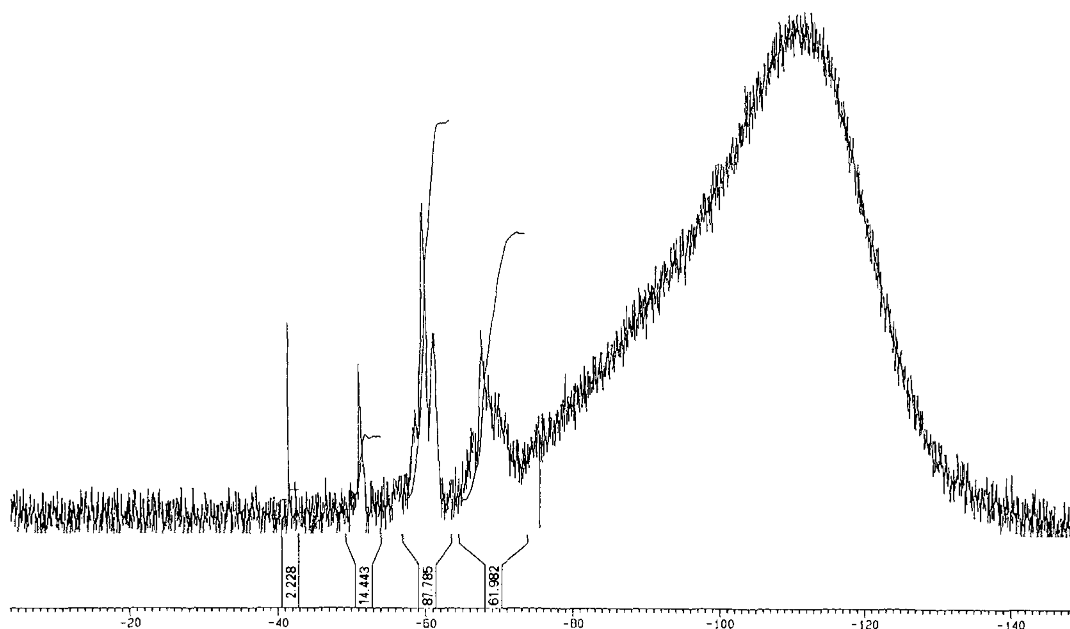


**Fig. 5.** $^{29}$Si NMR of PEO silane in $D_2O$.

of the region from wave number 2500 to 3500. A difference between the two spectra can clearly be seen in this region. For the coated powder, there is a strong peak at 2930 and a weak peak at 2850. These peaks corresponds to a $CH_2$ group. The literature suggests that a $CH_3$ group should give a strong peak at 2960 and a weak peak at 2875. There appears to be a shoulder at 2960 and the peak at 2875 is mainly covered by the two peaks of the $CH_2$ group.

### 4.3 XPS

Figure 7 shows the survey spectra with the PEO-film [Fig. 7(a)] and with the 'natural' surface contamination [Fig. 7(b)], both at a take-off angle of 45°. The intensity of both spectra were adjusted to a common scale with 1375 counts $s^{-1}$ and per division. The coverage with PEO silane results in a strong increase of the oxygen and carbon signal and a corresponding decrease in both the silicon and nitrogen signal intensities. For a better quantitative comparison, the integrated peak areas were divided by the appropriate atomic sensitivity factors. The ionization cross section and the transmission function of the spectrometer were taken

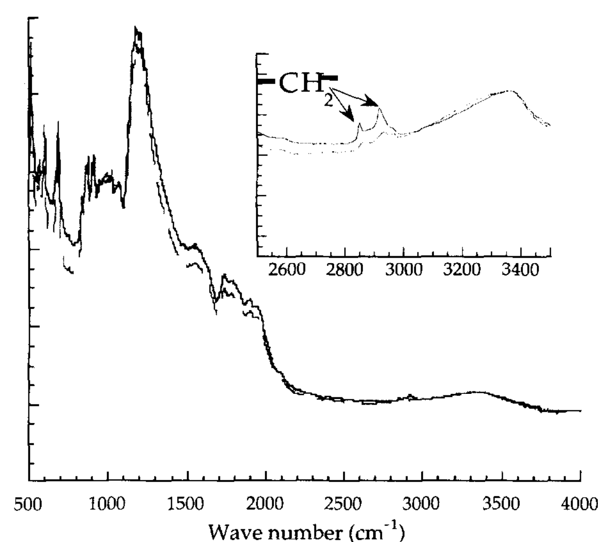


**Fig. 6.** DRIFT spectra of silicon powder with and without PEO silane.

into account. The atomic sensitivity factors were provided by Physical Electronics. The atomic concentration ratio of O1s/Si2p and Si2p/N1s are listed in Table 1. The atomic ratio of O1s/Si2p for the PEO-film is almost double that of the natural contamination layer. The atomic ratio of Si2p/N1s

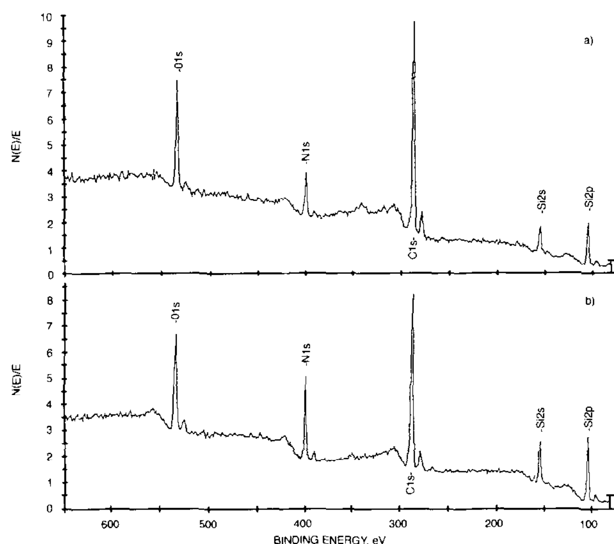


**Fig. 7.** XPS survey spectra of the $Si_3N_4$ substrate with (a) the PEO-filmand with (b) a natural contamination layer.

does not change drastically, 1·21 to 0·94. Sputter cleaning of the sample results in a decrease of the carbon and oxygen signal. The atomic ratio of Si/N also further decreases, but does not achieve the nominal concentration ratio of 0·75, indicating that the surface terminates with silicon coverage.

A detailed investigation of the different peaks show that the nitrogen peak is very sensitive to the chemical environment. In all figures, underground subtraction was carried out. All spectra were adjusted to a common y-axis with 975 counts $s^{-1}$ per division. In Fig. 8, peak no. 1 shows the nitrogen peak of the sputter cleaned $Si_3N_4$ substrate. It shows a nearly symmetric Gaussian peak shape, as it is expected from other measurements.[23,26] Peak no. 2 shows the nitrogen peak intensity of the same sample before the sputter cleaning procedure. Furthermore the main peak intensity shifts slightly ($\Delta E = 0{\cdot}4$ eV) toward a higher binding energy (BE)- (see Table 2). The coverage with the PEO-film results in a further decrease of the main intensity and an increase of the additional peak intensity (see no. 3). Again the main peak shifts slightly by ($\Delta E = 0{\cdot}2$ eV). As shown in Fig. 8 (insert), this nitrogen peak (no. 3) can be fitted very well with two Gaussian peaks. The higher intensity at lower BE will be denoted by N 1s(l) and the peak with the lower intensity at higher BE will be denoted as N 1s(h) and the sum as N 1s. The atomic ratios of Si2p, O1s, and N1s(l) are listed in Table 1 for the $Si_3N_4$ substrate coated with the organic film for various take-off angle ($\Psi$). Table 1 also lists the same atomic ratios for the untreated $Si_3N_4$ substrate for various sputtering time.

In order to measure the surface composition in the organic surface layer and on the underlying substrate, the take-off angle ($\Psi$), relative to the surface, was varied stepwise between 15° and 45°. The XPS-spectra for nitrogen (N1s(l) and N1s(h)) for various take-off angles are displayed in Fig. 9, $\Psi = 45°$ (spectrum no. 1), $\Psi = 15°$ (spectrum no. 3). Spectrum no. 2 shows the XPS-spectra at $\Psi = 15°$ several hours after XPS-measurement. It can clearly be seen, that the total intensity of N1s as well as the atomic ratio of N1s (l)/N1s (h) increases with increasing take-off angle (see Table 1).

The binding energies (BE) of the two nitrogen 1s levels and oxygen 1s do not change with the take-off angle. However, the BE of the Si 2p core level shifts with increasing take-off angle from 104·4 eV to 104·0 eV (see Table 2). Indicating that the Si2p peak is composed of peaks from different binding energies at different depths.

The N 1s(l) peak is attributed to nitrogen binded in the bulk $Si_3N_4$ material and N 1s(h) peak to nitrogen in a contamination layer on the surface (i.e. N binded to C and O). Table 1 shows that the ratio of N1s(l)/N 1s(h) peak areas is significantly less for the PEO coated substrate than for the untreated $Si_3N_4$ substrate with a contamination layer. Table 1 also shows that the ratio of the O1s/Si2p peak areas is higher for the PEO treated $Si_3N_4$ surface than the normal contaminated $Si_3N_4$ surface which suggests a thick oxygen layer on the bulk substrate. Both of these effects are attributed to the addition of a thin organic layer.

For the PEO coated substrate, the ratio of the O1s/Si2p peak areas decreases with increasing take off angle, equivalent to an increase in information depth. A clear indication that the Si is beneath a thick C and O-layer (i.e. the X group of the silane

**Table 1.** Atomic ratio of the elements Si, N, and O in untreated $Si_3N_4$ and PEO silane treated $Si_3N_4$

| | *O1s/Si2p (atomic-ratio)* | *Si2p/N1s (atomic ratio)* | *Si 2p/N 1s(h) atomic ratio* | *Si 2p/N 1s(1) atomi ratio* | *Nis (l)/N 1s(h)* |
|---|---|---|---|---|---|
| PEO-film on a $Si_3N_4$ substrate at a take-off angle of | | | | | |
| $\Psi = 15°$ | 2·055 | 3·24 | 7·57 | 5·22 | 1·450 |
| $\Psi = 30°$ | 1·691 | 1·64 | 6·49 | 2·17 | 2·993 |
| $\Psi = 45°$ | 1·281 | 1·21 | 6·32 | 1·55 | 4·078 |
| Sputter time of $Si_3N_4$-standard at a take-off angle of $\Psi = 45°$ | | | | | |
| 0 min | 0·77 | 0·94 | 8·63 | 1·86 | 8·144 |
| 24 min | 0·31 | 0·91 | 24·47 | 0·94 | 25·93 |

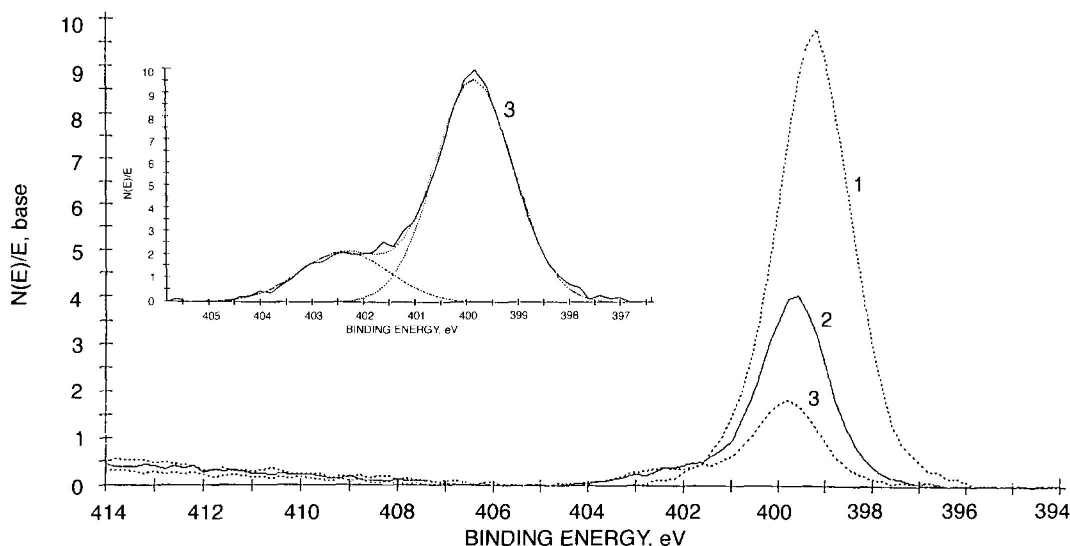


**Fig. 8.** XPS-Spectra of the nitrogen 1s peak for three different samplesurfaces: no. 1 for the sputter-cleaned $Si_3N_4$ substrate; no. 2 for $Si_3N_4$ substrate with a natural contamination layer; no. 3 for $Si_3N_4$ substrate with a PEO-film. In the small inserted picture the nitrogen spectrum no. 3 is magnified and deconvoluted with two Gaussian shaped peaks. The two different peaks are denoted as N1s (l) and N1s (h).

molecule is pointing away from the surface). This assumption also agrees with the angle dependence of the atomic ratio of N1s(l)/N1s(h) as well as with the angle dependence of the atomic ratio of Si2p/N1s(l) (see Table 1). The nitrogen bonded in the bulk is beneath the nitrogen bonded in the polymer and the Si which is at the interface between substrate and polymer. Consequently, one would expect an increase in the ratio of the Si 2p/N 1s(h) peak areas with increasing information depth. However, Table 1 shows the ratio does not change but actually decreases a small amount. This unexpected result is attributed to an attenuation effect. Due to the different kinetic energies of the emitted photoelectrons ($E_{Si} > E_N > E_O$), the mean free path of Si is higher than for nitrogen and thus the information depth for Si is higher than for N. Therefore, already for a small take-off angle, more signal emitted from the silicon layer just beneath the nitrogen-polymer-layer than emitted from the nitrogen in the PEO layer arrives at the analyzer. Hence, increasing the take-off angle leads to an unproportional increase of the nitrogen signal resulting in a slight decrease of the concentration ratio.

**Table 2.** Binding energies of the Si2ps, N1s(l) and N1s(h) peak intensities in untreated $Si_3N_4$ and PEO silane treated $Si_3N_4$. See Section 4·3 for definitions of N1s (l) and N1s (h)

| | *BE Si2p* | *BE O1s* | *BE N1s* |
|---|---|---|---|
| PEO-film on a $Si_3N_4$ substrate at a take-off angle of | | | |
| $\Psi = 5°$ | 104·4 | 434·8 | 399·8 |
| $\Psi = 30°$ | 104·2 | 534·8 | 399·8 |
| $\Psi = 45°$ | 104·2 | 534·8 | 399·8 |
| Sputter time of $Si_3N_4$-standard at a take-off angle of $\Psi = 45°$ | | | |
| 0 min | 103·8 | 534·6 | 399·6 |
| 1 min | 103·4 | 533·6 | 399·2 |
| 24 min | 103·2 | 533·8 | 399·2 |

### 4.4 UV adsorption isotherm

The adsorption isotherm of PEO silane on silicon nitride powder using UV techniques is shown in Fig. 10. The measurements were severely hampered by dissolution of ammonia from the surface. The ammonia, being UV active at the same wavelength, caused higher UV reading than the calibration curve would predict. Therefore, it was only possible to determine when all PEO silane added adsorbed to the surface of the powder (point E in Fig. 10) and when the maximum adsorbed amount had been achieved (< F in Fig. 10). Point E was determined by comparing the measured value to that of the supernate of silicon nitride powder dispersed in water without PEO silane. Point F was calculated by determining the point at which the UV adsorption increased linear with increasing PEO silane concentration. Point E and F correspond to adsorbed amounts of $0{\cdot}052\,\mu mol\,m^{-2}$ and $0{\cdot}104\,\mu mol\,m^{-2}$, respectively. The value of F is determined by assuming that all the PEO silane added between the concentrations generating points E and F adsorbs. The saturation concentration is approximately $5 \times 10^{-5}\,g\,ml^{-1}$. Samples allowed to equilibrate for 2 weeks yielded the same experimental results.

### 4.5 Ellipsometry

The kinetics of the adsorption of PEO silane on silicon nitride was too slow to allow the determination of an adsorption isotherm curve. In

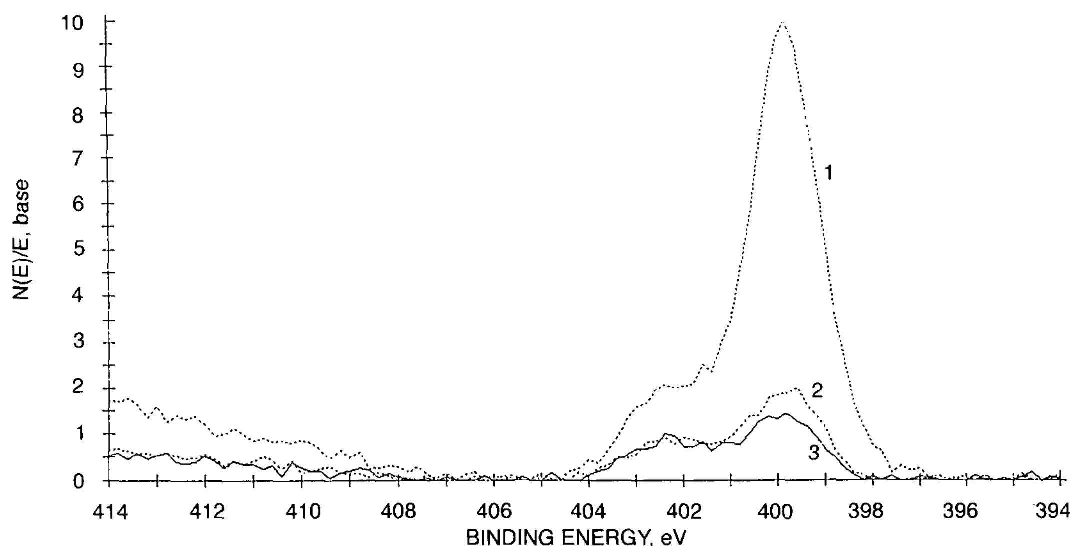


**Fig. 9.** XPS-spectra of the nitrogen 1s peak at two take-off angles Ψ, relative to the surface: no. 1 for Ψ = 45°, no. 2 for Ψ = 15° after X-ray bombardment for several hours and no. 3 for Ψ = 15° at the beginning of the angle resolved XPS data acquisition.

addition, solution of the Fresnel equations for the system was not possible. Only measurement of the maximum adsorbed amount was possible. Figure 11 shows a plot of the optical parameter Δ, related to film thickness, as a function of time. Point A and B correspond to the addition of 5 ml of $1 \times 10^{-1}$ g ml$^{-1}$ PEO silane solution at pH 10. For this large concentration the adsorption was rapid. The maximum adsorbed amount for the 5 samples explored was determined to be 2·1 $\mu$mol m$^{-2}$ (±0.5).

### 4.6 AFM

Figure 12 shows the interparticle potential between $Si_3N_4$ in water at pH 10 with and without PEO silane. At pH 10 silicon nitride has a very high surface charge and thus a long range repulsive force. Figure 12 shows that the silane coated system experiences a longer range repulsive force then the untreated $Si_3N_4$ sample.

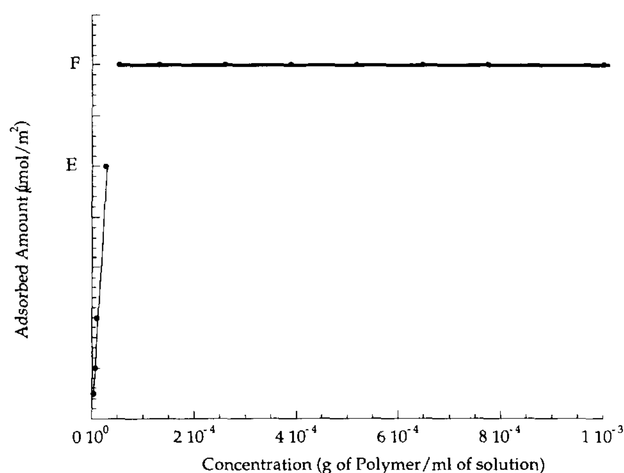


**Fig. 10.** UV determined adsorption isotherm. Point E and F correspond to adsorbed amounts of 0·052 $\mu$mol m$^{-2}$ and 0·104 $\mu$mol m$^{-2}$, respectively (see text).

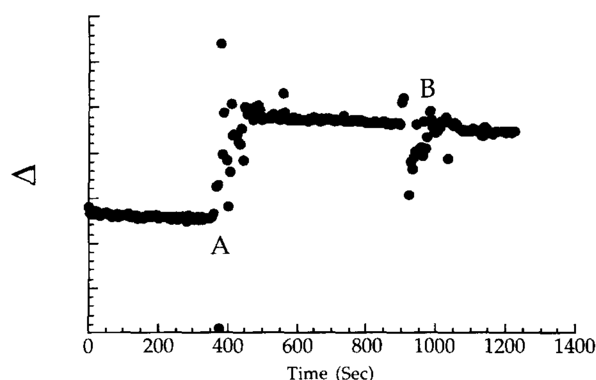


**Fig. 11.** Ellipsometry determined adsorption isotherm.

## 5 Discussion

The $^{29}Si$ NMR spectra of the starting compound in THF $d_8$ (Fig. 3) shows that it is extremely stable with regards to polycondensation. No special storage or handling conditions (e.g. glove box, glove bag, nitrogen storage) are used and still after months of use the compound does not polymerize. Figure 5 shows that upon the addition of water and acid polycondensation reactions occur. Only 1% of the starting material remains in the solution after 24 h.

The structure of the PEO silane compared with that of the surface of $Si_3N_4$ is such that the only surface groups detectable by DRIFT are CO, $CH_2$ and $CH_3$. The surface of silicon nitride already has Si–O and N–H bonds and thus it is extremely difficult if not impossible to measure an increase in this quantity caused by the chemical binding of the silane molecule to the surface. Therefore, DRIFT measurements could confirm that the PEO silane is strongly bonded to the surface but could not

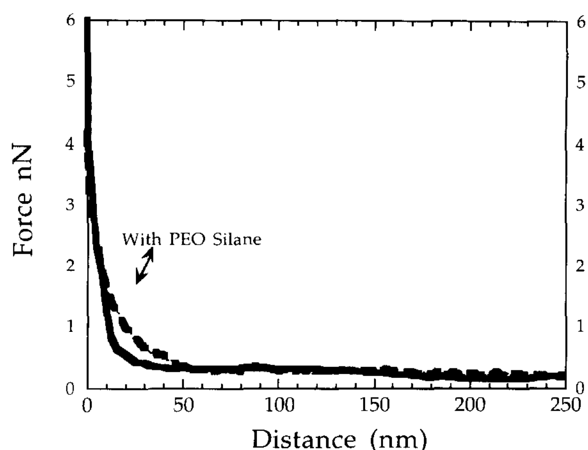


**Fig. 12.** Comparison of AFM results for $Si_3N_4$ coated with ($1e\text{-}3\,g\,ml^{-1}$) and without PEO Silane.

confirm whether the silane molecule is physically bound or chemically grafted. Presence of $CH_3$ groups in the DRIFT spectra indicate that there are still unreacted alkoxy groups on the PEO silane molecule.

XPS results confirm the presence of the PEO silane molecule on the $Si_3N_4$ substrate. The vacuum pressure of the UHV chamber, $3\times10^{-7}$ Pa, is an indication of how strongly the molecule is bonded. The XPS results clearly show that the silane end of the molecule is adjacent to the silanol rich $Si_3N_4$ surface. For thermodynamic reasons, two SiOH bonds in immediate proximity will react to form an Si–O–Si bond and thus we can conclude that the PEO silane molecule chemically binds to the surface of $Si_3N_4$. It is possible that the PEO silane molecule can form covalent bonds with the Si-N bonds on the surface of $Si_3N_4$, but it is not thermodynamically favored.

The maximum adsorbed amount determined by UV spectroscopy and ellipsometry differ by a factor of 20. This strongly indicates that the PEO silane molecule not only chemically binds, but also physically binds to the surface. The physically bonded molecules are removed during centrifugation giving the lower maximum adsorbed amount by UV adsorption. Buchta *et al.*[15] came to a similar conclusion by different experimental methods. They suggested that the silane end when adjacent to the silicon nitride surface forms a chemical bond and the X polymer chain when adjacent to the surface forms a physical bond. In the case of the PEO silane molecule. The terminating alcohol group forms a hydrogen bond with the silicon nitride surface groups. Thus, the PEO silane molecule is only physically bonded when the PEO chain is adjacent to the silicon nitride surface. AFM results presented here and the rheology results of Colic *et al.* show that this trace amount of silane molecule is adequate to improve the dispersability of the powder.

## 6 Conclusions

Diffuse reflectance infrared fourier transform (DRIFT) spectroscopy showed that PEO silane is strongly bonded to the surface of silicon nitride. X-Ray photoelectron spectroscopy (XPS) was able to determine that the PEO silane is chemically grafted to the surface. UV spectroscopy and ellipsometry measurements were able to determine that the amount of chemically grafted PEO silane is very small. The majority of the PEO silane is physically bonded to the $Si_3N_4$ surface. AFM results show that even a small amount of PEO silane on the surface of silicon nitride has a beneficial effect on the interparticle forces. Thus, the large amount of physically bonded PEO silane leads to the reduction in the rate of silica dissolution[16] and the small amount of chemically bonded compound prevents particles from being pushed into the deep potential well during consolidation.[16]

## References

1. Tanaka, H., A recent tendency of $Si_3N_4$ cutting tools. *Trans. Mater. Res. Soc. Jpn.*, 1994, **14A**, 541–545.
2. Mitomo, M. and Petzow, G., Recent progress in silicon nitride and silicon carbide ceramics. *MRS Bulletin*, 1995, **20**(2), 19–20.
3. Lange, F. F., Powder processing science and technology for increased reliability. *J. Am. Ceram. Soc.*, 1989, **72**, 1–3,15.
4. Aksay, I. A., Microstructure control through colloidal consolidation. In *Advances in Ceramics, Vol. 9, Forming of Ceramics*, ed J. A. Mangels and G. L. Messing. American Ceramic Society, Columbus, OH, 1984, pp. 94–104.
5. Chang, J. C., Velamakanni, B. V., Lange, F. F. and Pearson, D. S., Centrifugal consolidation of $Al_2O_3$ and $Al_2O_3$/$ZrO_2$ composite slurries vs. interparticle potentials: particle packing and mass segregation. *J. Am. Ceram. Soc.*, 1991, **74**, 2201–2204.
6. Chang, J. C., Lange, F. F., Pearson, D. S. and Pollinger, J. P., Pressure sensitivity for particle packing of aqueous $Al_2O_3$ slurries vs interparticle potential. *J. Am. Ceram. Soc.*, 1994, **77**(5), 1357–1360.
7. Velamakanni, B. V., Chang, J. C., Lange, F. F. and Pearson, D. S., New method for efficient colloidal particle packing via. modulation of repulsive lubricating hydration forces. *Langmuir*, 1990, **6**, 1323–1325.
8. Leong, Y. K. and Boger, D. V., Surface chemistry effects on concentrated suspension rheology, *J. Colloid and Interface Science*, 1990, **136**(1), 249–258.
9. Rueb, C. J. and Zukoski, C. F., Viscoelastic properties of colloidal gels. *J. Rheol.*, 1997, **41**(2), 197–218.
10. Yanez, J. A., Shikata, T., Lange, F. F. and Pearson, D. S., Shear modulus and yield stress measurement of attractive alumina particle networks in aqueous slurries. *J. Am. Ceram. Soc.*, 1996, **79**(11), 2917–2924.
11. Israelachvili, J., *Intermolecular and Surface Forces*, 2nd edn. Academic Press, San Diego, CA 1991.
12. Russel, W. B., Saville, D. A. and Schowalter, W. R., *Colloidal Dispersions*. Cambridge University Press, New York, 1989.
13. Luther, E. P., Kramer, T. M., Lange, F. F. and Pearson, D. S., Development of short-range repulsive potentials in aquesous silicon nitride slurries. *J. Am. Ceram. Soc.*, 1994, **77**(4), 1047–1051.

14. Kramer, T. and Lange, F. F., Rheology and particle packing of chem- and phys-adsorbed, alkylated silicon nitride powders. *J. Am. Ceram. Soc.*, 1994, **77**(4), 922–928.
15. Buchta, M. A. and Shih, W., Improved aqueous dispersion of silicon nitride with aminosilanes. *J. Am. Ceram. Soc.*, 1996, **79**(11), 2940–2946.
16. Colic, M., Franks, G. V., Fisher, M. and Lange, F. F., Development of short range repulsive inter-particle forces in aqueous $Si_3N_4$ slurries with chem adsorbed silanes. *J. Am. Ceram. Soc.*, in press.
17. Plueddemann, E. P., *Silane Couling Agents*, 2nd edn. Plenum Press, New York, 1991.
18. Vrancken, K. C., Possemiers, K., Van Der Voort, P. and Vansant, E. F., Surface modification of silica gels with aminoorganosilanes. *Colloids and Surfaces*, 1995, **98**, 235–241.
19. Yuan, W. and Van Ooij, W. J., Characterization of organofunctional silane films on zinc substrates. *J. Coll. and Inter. Sci.*, 1997, **185**, 197–209.
20. Whitman, P. K. and Feke, D. L., Colloidal charaterization of ultrafine silicon carbide and silicon nitride powders. *Adv. Ceram. Mater.*, 1986, **1**(4), 366–370.
21. Crimp, M. J., Johnson, R. E. Jr., Halloran, J. W., Feke, D. L., Colloidal behavior of silicon carbide and silicon nitride. In *Proceedings of Cimtec V.*, ed. L. L. Hench and D. R. Ulrich, Wiley, New York, 1989, pp.735–742.
22. Briggs, D. and Seah, M. P., *Practical Surface Analysis*, Vol. 1. John Wiley and Sons, 1990.
23. Löbau, J., Rumphorst, A., Galla, K., Seger, S. and Wolfrum, K., Adsorption of alkyl-trichlorosilanes on glass and silicon: a comparative study using sum-frequency spectroscopy and XPS. *Thin Solid Films*, 1996, **289**, 272–281.
24. Garbassi, F., Balducci, L., Chiurlo, P. and Deiana, L., A study of surface modification of silica using XPS. *Applied Surface Science*, 1995, **84**, 145–151.
25. Ducker, W. A., Sendon, T. J. and Pashley, R. M., *Langmuir*, 1994, **8**, 2527.
26. *Hand Book of X-ray Photoelectron Spectroscopy*, Ch. 9, ed. Jill Chastain. Perkin-Elmer Corporation, MN, 1992.